HHS Public Access

Author manuscript

Dev Cell. Author manuscript; available in PMC 2020 December 16.

Published in final edited form as:

Dev Cell. 2019 December 16; 51(6): 675–683.e4. doi:10.1016/j.devcel.2019.11.002.

Isl1 regulation of Nkx2.1 in the early foregut epithelium is required for tracheaesophageal separation and lung lobation

Eugene Kim[1,2], **Ming Jiang**[3], **Huachao Huang**[1], **Yongchun Zhang**[1], **Natalie Tjota**[1], **Xia Gao**[1], **Jacques Robert**[4], **Nikesha Gilmore**[5], **Lin Gan**[6], **Jianwen Que**[1,2,*]

[1]Division of Digestive and Liver Diseases, Department of Medicine, Columbia University Medical Center, New York, NY 10032, USA

[2]Columbia Center for Human Development, Columbia University Medical Center, New York, NY 10032, USA

[3]Institute of Genetics, The Children's Hospital, Zhejiang University School of Medicine, Hangzhou, Zhejiang 310058, China

[4]Department of Microbiology and Immunology, University of Rochester, Rochester, NY 14642, USA

[5]Department of Surgery, Cancer Control Division Geriatric Oncology, University of Rochester, Rochester, NY 14642, USA

[6]Department of Ophthalmology and Flaum Eye Institute, University of Rochester, Rochester, Rochester, NY 14642, USA

Summary

The esophagus and trachea arise from the dorsal and ventral aspects of the anterior foregut, respectively. Abnormal trachea-esophageal separation leads to the common birth defect esophageal atresia with/without tracheoesophageal fistula (EA/TEF). Yet the underlying cellular mechanisms remain unknown. Here, we combine *Xenopus* and mouse genetic models to identify that the transcription factor Isl1 orchestrates tracheaesophageal separation through modulating a specific epithelial progenitor cell population (midline epithelial cells-MECs, Isl1+ Nkx2.1+ Sox2+) located at the dorsalventral boundary of the foregut. Lineage tracing experiments show that MECs contribute to both tracheal and esophageal epithelium, and Isl1 is required for Nkx2.1 transcription in MECs. Deletion of the chromosomal region spanning the *ISL1* gene has been found in patients with abnormal trachea-esophageal separation. Our studies thus provide definitive

*Correspondence: BB 801A, 650 West 168th Street, Columbia University Medical Center, New York, NY 10032. TEL: 212-305-5961. jq2240@cumc.columbia.edu. Lead Contact and Lead Communication Contact: Jianwen Que, BB 801A, 650 West 168th Street, Columbia University Medical Center, New York, NY 10032. TEL: 212-305-5961. jq2240@cumc.columbia.edu.

Author Contributions

E.K. and J.Q. conceived the study, designed and performed the experiments, and wrote the manuscript. M.J., H.H., Y.Z., N.T., X.G. and N.G. performed the experiments. J.R. and L.G. provided intellectual contributions.

Declaration of Interests

The authors declare no competing or financial interests.

evidence that *ISL1* is a critical player in the process of foregut morphogenesis, acting in a small progenitor population of boundary cells.

Graphical Abstract

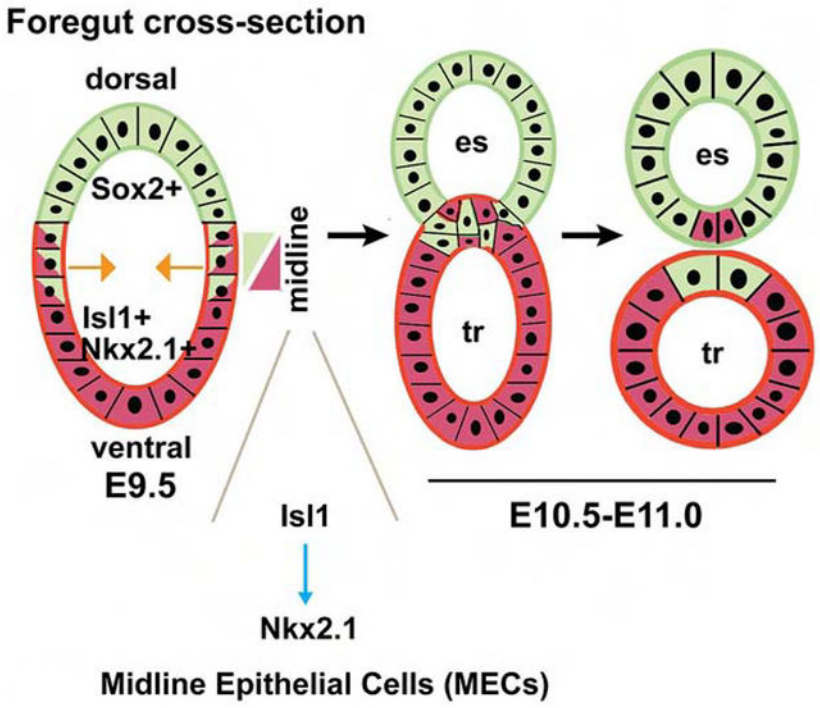

eTOC:

The disease mechanism of the birth defect esophageal atresia with/without tracheoesophageal fistula remains largely unknown. Kim et al. used Xenopus and mouse genetic models to show that an Isl1-Nkx2.1 axis regulates a midline epithelial progenitor cell population that orchestrates tracheo-esophageal separation.

Keywords

esophageal atresia; EA/TEF; Isl1; lung development

Introduction

Generation of the trachea and esophagus from the early foregut tube requires the coordinated function of multiple signaling pathways and transcription factors that are expressed in specific domains along the dorsal-ventral axis (Goss et al., 2009; Harris-Johnson et al., 2009; Minoo et al., 1999; Morrisey and Hogan, 2010; Que, 2015; Que et al., 2006; Que et al., 2007). For example, Wnt2/2b, Bmp4 and Nkx2.1 are enriched in the ventral foregut that will give rise to the trachea and lungs (Domyan et al., 2011; Goss et al., 2009; Minoo et al., 1999; Que et al., 2006). By contrast, the BMP signaling inhibitor Noggin and the transcription factor Sox2 are preferentially expressed in the dorsal foregut that gives rise to

the esophagus (Que et al., 2006; Que et al., 2007). Mouse genetic studies have shown that disruption of this expression pattern leads to abnormal trachea-esophageal separation (Domyan et al., 2011; Goss et al., 2009; Harris-Johnson et al., 2009; Malmstrom et al., 2008; Minoo et al., 1999; Morrisey and Hogan, 2010; Que, 2015; Que et al., 2006; Que et al., 2007). The resulting phenotypes recapitulate the common birth defect Esophageal Atresia with/without Trachea-Esophageal Fistula (EA/TEF) which affects approximately 1 in 3000 newborns (Fragoso and Tovar, 2014; Malmstrom et al., 2008). However, the cellular mechanisms regulating trachea-esophageal separation remain largely unknown.

Recent studies have shown that the dorsal-ventral patterning of some signaling pathways and transcription factors is conserved in the *Xenopus* foregut during trachea esophageal separation. For example, Sox2 and Nkx2.1 are respectively enriched in the epithelium of dorsal and ventral foregut of *Xenopus* embryos and their loss leads to abnormal separation of the trachea from the esophagus (Rankin et al., 2016; Rankin et al., 2015). These findings suggest a conserved genetic mechanism controlling foregut development in both mouse and frog embryos. Here, we took advantage of this conserved developmental mechanism to identify the transcription factor Isl1 as a critical player regulating trachea-esophageal separation. Significantly, we find an epithelial progenitor population that co-expresses Sox2, Nkx2.1 and Isl1 in the dorsal-ventral boundary of the anterior foregut. Our lineage tracing studies demonstrate that this unique population contributes to both tracheal and esophageal epithelium. Deletion of *Isl1* in this population results in the formation of EA/TEF. Our further analysis suggests that Isl1 regulates expression of Nkx2.1 in these epithelial progenitor cells.

Results

A screen of dorsal-ventral differentially expressed transcription factors identifies *Isl1* as a regulator of trachea-esophageal separation

In mouse, the trachea and esophagus are separated approximately at embryonic (E) 9.5-E11.5. Some genes including *Sox2* and *Nkx2.1* continue to be differentially expressed in the nascent trachea and esophagus right after separation (at E11.5) (Figure 1A). We reasoned that comparison of genes differentially expressed in the E11.5 esophagus and trachea can provide us leading information about dorsal-ventral differential genes in the E9.5 foregut. To identify genes potentially playing a role in foregut morphogenesis we performed microarray analysis using tracheas and esophagi isolated from the mouse embryo soon after separation at E11.5 (n=3 for each group). 187 genes were differentially expressed in the two tissues (≥1.5 fold, Table S1). Annotation using PANTHER (Protein Analysis Through Evolutionary Relationships) identified a significant number of genes encoding components of biological processes such as developmental regulation, cell adhesion, matrix composition and remodeling, proliferation and cell growth, some of which have already been implicated in foregut morphogenesis (Figures 1B and S1A) (Fausett et al., 2014; Li et al., 2007; Que et al., 2006). As expected, genes such as *Sox9*, *Wnt7b*, and the BMP signaling downstream targets *Id1*, *Id3* are preferentially expressed in the respiratory organs (Table S1)(Hines et al., 2013; Jen et al., 1996; Rajagopal et al., 2008; Shu et al., 2002). Conversely, the transcript levels of genes including *Pitx1*, *Sox21*, *Sox2* and *p63* are enriched in the E11.5 esophagus (Table S1)

(Que et al., 2009; Zhang et al., 2016). Results from the microarray analysis were confirmed by qPCR and immunostaining (Figures 1A, C-D and S1B).

Among the differentially expressed genes we identified 32 that encode transcription factors (Table 1). Survey of the literature definitively excluded EA/TEF as a null mutant phenotype of most of these genes (Table 1). However, no information is available for Isl1 and Sall1. Isl1 was of particular interest because we found that it is expressed in the epithelium and mesenchyme of the mouse trachea but not the esophagus at E11.5 (Figure 1E). In addition, at E9.5 Isl1 expression is limited to the epithelium and mesenchyme of the ventral foregut where the trachea arises (Figure 1F and S1C). We also noted that epithelial cells located at the dorsal-ventral boundary in the E9.5 foregut co-express Isl1 and Sox2 (Figure 1F and S1C).

We therefore tested the function of Isl1 (as well as Sall1) using morpholino knockdown in the *Xenopus laevis* embryo. We included two controls, Ovol2 (Ovo Like Zinc Finger 2), a transcription factor not differentially expressed and Mrpl24 (mitochondrial ribosomal protein L24), a protein ubiquitously expressed. Embryos were injected with antisense morpholinos at the 16-cell stage and analyzed after hatching at developmental stage 41. This stage was chosen because prior studies had shown that Sox2 and Nkx2.1 are differentially expressed at 50 hpf (stage 36) before separation (Rankin et al., 2016), and that this pattern is maintained after the completion of tracheaesophageal separation at state 41 (Figures 1G and S1D). As expected, we found that morpholino-mediated knockdown of *Nkx2.1* led to abnormal separation (Rankin et al., 2016). Knockdown of Sall1, Ovol2 and Mrpl24 did not cause abnormal tracheaesophageal separation (at least 12 for each, data not shown). By contrast, knockdown of *Isl1* disrupted *X. laevis* trachea-esophageal separation (n=8/14, Figure 1H).

Isl1 deletion leads to EA/TEF and lung lobe fusion in *Shh-Cre;Isl1*$^{loxp/loxp}$ mouse mutants

Given this finding with *X. laevis* embryos we proceeded to investigate the role of isl1 in mouse foregut development. Isl1 is a LIM homeodomain transcription factor critical for the development of multiple organs including the pancreas and heart (Ahlgren et al., 1997; Bu et al., 2009; Cai et al., 2003; Cho et al., 2014; Moretti et al., 2006; Pan et al., 2008). *Isl1* null mutants die at approximately E10.5 due to severe heart problems (Ahlgren et al., 1997). Thus far the role for *Isl1* in foregut development remains undetermined. At E9.5 Isl1 expression is limited to the epithelium and mesenchyme of the ventral foregut (Figure 1F). Following the completion of trachea-esophageal separation, Isl1 is expressed in the trachea but not the esophagus (Figure 1E). While Isl1 remains to be highly expressed in the ventral epithelium and mesenchyme of the trachea at E13.5 (Figure S2C), low levels of Isl1 are detected in the epithelium of the budding lung tips (Figure S2D). At E14.5 Isl1 expression in the lung epithelium falls below detectable levels although Isl1 remains to be expressed in the mesothelium (Figure S2A). We generated *Shh-Cre;Isl1*$^{loxp/loxp}$ mutants where *Isl1* is deleted in the foregut endoderm prior to trachea-esophageal separation. At E9.5-E10.5 *Shh-Cre* is specifically active in the ventral foregut epithelium as evident by the lacZ reporter activities in *Shh-Cre;R26*^{lacz} embryos (Figure S2B). In line with this finding Isl1 expression is lost in the epithelium of the ventral foregut in E9.5 *Shh-Cre;Isl1*$^{loxp/loxp}$ mutants (n=9, Figure 2A),

and the expression is also lost in the epithelium of the trachea and lung at E13.5 (Figure S2C,D). Mutants die at birth likely due to issues in other organs such as heart and brain where *Shh-Cre* is also active. Significantly, approximately 50% (18/36) of all mutants examined at various embryonic stages demonstrate abnormal separation of the trachea and esophagus, leading to the formation of proximal EA with distal TEF (Figure 2B). Although Isl1 has been shown to regulate the proliferation of pharyngeal endodermal cells (Cai et al., 2003), the proliferation of epithelial progenitor cells for trachea and esophagus seems unaffected in *Shh-Cre;Isl1*$^{loxp/loxp}$ mutants at E9.5 and E10.5 (at least 3 pairs of mutants and controls for each timepoint, $p>0.05$, Figure S3A). We also examined apoptotic cells with cleaved caspase 3 and did not observe significant changes between mutants and controls at E9.5 and E10.5 (Figure S3B and data not shown). In addition, we deleted *Isl1* in the mesenchyme with *Dermo1-Cre* and did not observe abnormal separation of the trachea and esophagus, although the right lung lobes appear dysmorphic (n=7, Figure S3C).

Deletion of *Isl1* with *Shh-Cre* caused the fusion of all four right lung lobes in all mutants (36/36) (Figure 2C). Branching morphogenesis seems delayed in all mutants when examined at E13.5 (Figure S3D). Notably, EA/TEF is often associated with lung lobe fusions (e.g. horseshoe lung) and long-term respiratory problems in patients (Legrand et al., 2012; Sistonen et al., 2010; Wales et al., 2002). We therefore determined whether loss of Isl1 affected the differentiation of lung epithelium. In the intrapulmonary airways the numbers of club and ciliated cells are not significantly different between mutants and controls (Figure 2C). In addition, loss of Isl1 did not affect the development of alveolar cells (type I cells-T1a, type II cells-SpC)(Figure 2C). Together these results suggest that Isl1 is required for trachea-esophageal separation. Our data also demonstrate that Isl1 regulates lung lobation but not epithelial differentiation.

Isl1 in a midline epithelial population (Nkx2.1+ Isl1+ Sox2+) located at the dorsalventral boundary foregut is critical for trachea-esophageal separation and lung lobation

We previously showed that the midline epithelium moves towards the center of the lumen to form a septum that divides the anterior foregut into the trachea and esophagus (Figures 3A–B and S4A–B)(Que, 2015; Que et al., 2006). Formation of the septum involves cell intercalation and some Nkx2.1+ cells incorporate into the ventral epithelium of the nascent esophagus (1~2 Nkx2.1+ cells per cross-section, Figures 3A–C and S4A–C). Notably, Isl1+ cells are also present in the nascent esophagus (Figure 3D), and Sox2+ cells are present in the dorsal epithelium of the nascent trachea (Figures 3C–D). To confirm the contribution of Nkx2.1+ cells to the esophageal epithelium we performed lineage tracing using a knockin *Nkx2.1-CreER* mouse line. When a single dose of Tamoxifen was given at E8.5 (prior to foregut separation), a cluster of Xgal+ epithelial cells were observed in the ventral epithelium of the esophagus (Figures 3E–F). By contrast, when two doses of Tamoxifen were injected at E8.5 and E9.5, clusters of Xgal+ epithelium are present in two separate spots (n=3, Figures 3G and S4D), suggesting that each injection induces genetic recombination in a short-time window and that Nkx2.1 expression is transient in these esophageal cells (Figures 3G and S4D). The findings confirmed that a small number of Nkx2.1+ airway epithelial cells incorporate into the esophagus during trachea-esophageal separation. In addition, in the same littermates Xgal+ spots are located in the stomach of

some embryos (Figure S4D), suggesting that lung-stomach separation occurs prior to trachea-esophageal separation. By contrast, when Tmx is administrated at E10.5, no Xgal+ cells were observed in the esophagus (Figure S4E), further confirming that Nkx2.1 expression is transient.

Since Isl1 is also expressed in the septum formed by the midline epithelial cells (MECs, Nkx2.1+ Isl1+ Sox2+ (Figure 3D), we asked whether Isl1 expression there is critical for the separation process. We addressed this issue by using a *Sox2-CreER* knockin mouse line which only targets the dorsal and MECs when a single low dose of Tamoxifen was injected at early E8.5 (Figure 4A). Lineage labeled epithelial cells intercalate to form the septum at E10.5 and contribute to the dorsal epithelium of the trachea (Figure 4A). Significantly, EA/TEFs develop in 100% *Sox2-CreER;Isl1*$^{loxp/loxp}$ mutants (n=9, Figures 4B and S4F), confirming that Isl1 expression in the MECs is critical for trachea-esophageal separation. In addition, all of the *Sox2-CreER;Isl1*$^{loxp/loxp}$ mutants present fusion of right lung lobes (Figure S4G).

Isl1 regulates expression of Nkx2.1 in MECs during trachea-esophageal separation

We next examined expression of Nkx2.1 and Sox2 in the boundary epithelial population following *Isl1* deletion. We found that the levels of Sox2 are moderately reduced (Figures 4C–D). By contrast, the levels of Nkx2.1 were dramatically reduced in the MECs of *Shh-Cre;Isl1*$^{loxp/loxp}$ mutants at E9.5 (Figure 4C). Notably, the levels of Nkx2.1 in some ventral epithelial cells are also reduced which may contribute to the lung lobation defect (Figures 4C). Consistent with the potential regulation of Nkx2.1 by Isl1, the levels of Nkx2.1 are also decreased in the MECs of *Sox2-CreER;Isl1*$^{loxp/loxp}$ mutants following Tamoxifen induction (Figure 4D).

To further test whether Isl1 regulates the transcription of Nkx2.1 we examined the regulatory region of the *Nkx2.1* gene. One Isl1 consensus binding motif (*TAAT*) was identified within the 400bp *Nkx2.1* promoter element (Figure 4E). To assess whether this region is critical for the transcription regulation of Nkx2.1, we performed luciferase assays in two cell lines, the immortalized mouse lung epithelial cell line MLE-15 which expresses the *Nkx2.1* gene and the hamster islet cell line HIT-T15. Transfection of Isl1 expressing plasmids leads to a significant increase in the luciferase activities in both cell lines (Figure 4E). Conversely, mutation of the potential binding site (TAAT → GCCG) abolishes the transcription regulation (Figure 4F). We further confirmed that Isl1 binds to the regulatory region of the *Nkx2.1* gene using Chromatin Immunoprecipitation (ChIP) assay. Significant enrichment of Isl1 was observed (approximately three folds) as detected by ChIP-PCR (Figure 4G). Together these findings support that Isl1 regulates the transcription of Nkx2.1 during trachea-esophageal separation.

Discussion

Generation of the esophagus and trachea from the early anterior foregut involves cell movement, coordinated cell proliferation and differentiation. Here, we used a combined frog and mouse genetic models to identify the transcription factor Isl1 as a regulator of trachea-esophageal separation. We also defined a dorsal-ventral boundary epithelial progenitor

population (MECs, Isl1+ Sox2+ Nkx2.1+) which contributes to both tracheal and esophageal epithelium. Deletion of *Isl1* in this population leads to the formation of EA/TEF and lung lobation defects. Our further analysis revealed that Isl1 is required for Nkx2.1 expression in these midline cells.

Conserved molecular mechanisms regulating trachea-esophageal separation in Xenopus and mouse embryos

Frog and mouse foregut share similar expression of multiple signaling molecules and transcription factors (Rankin et al., 2016; Rankin et al., 2015). In the accompanying manuscript Dr. Zorn group further confirms the conserved function of Shh/Gli signaling in foregut morphogenesis (Nasr et al.). Here, we found that blocking Isl1 function results in abnormal separation in both frog and mouse embryos. Our studies emphasize that the combined use of frog and mouse genetic models is powerful for identifying players in the regulation of foregut morphogenesis. Along this line our microarray data include genes regulating cell-cell adhesion, matrix production which have been linked to trachea-esophageal separation (Fausett et al., 2014; Li et al., 2007; Que et al., 2006). Interestingly, some of these genes (e.g. troponin I type 1 (*Tnni*)) contain Isl1 binding sites (Table S2), and in the future it will be interesting to test the function of these genes during foregut morphogenesis using genetic manipulations in combined animal models.

Lineage tracing indicates that respiratory cells contribute to the esophageal epithelium

Our immunohistological study suggests a mixing of epithelial progenitor cells during the formation of the septum (barrier) to divide the anterior foregut into the trachea and esophagus. In this process, the MECs (Isl1+ Nkx2.1+ Sox2+) in the dorsal-ventral boundary region moves towards the center from the lateral sides, involving epithelial intercalation and incorporation. Our lineage tracing results demonstrate that some Nkx2.1+ lineage-derived epithelial cells incorporate into the epithelium of the esophagus and lesser curvature of the stomach. Our data further suggest that expression of Nkx2.1 in the esophageal epithelium is transient. Otherwise a stream of lineage labeled cells should be observed. Presence of the MECs-derived cells in the esophagus is intriguing in that these cells may offer an etiology explanation of inlet patch, which is a congenital anomaly characterized by the presence of columnar cells in the esophagus, especially in the upper part of the tube (Di Nardo et al., 2016). Inlet patch can produce acid like the gastric tissue and is found in up to 10% of the population undergoing endoscopy inspection. Consistent with our lineage tracing data, inlet patches are mostly solitary and extend longitudinally, affecting only part of the circumference (Behrens and Yen, 2011). It is possible that the boundary population-derived cells fail to switch off the respiratory genes like *Nkx2.1* and partially maintain the columnar cell identity, giving rise to the columnar cells in the inlet patches. Conversely, a recent study has shown that downregulation of *Nkx2.1* leads to the expression of gut genes in the lung alveolar epithelium (Tata et al., 2018). In this study it is possible that the epithelium amenable to fate switch is originated from the gastric tissue during lung-stomach/esophageal separation.

Isl1 function in foregut morphogenesis

Isl1 is critical for the development of multiple tissues including pancreas and brain (Ahlgren et al., 1997; Bu et al., 2009; Cai et al., 2003; Cho et al., 2014; Moretti et al., 2006; Pan et al., 2008). We found that deletion of *Isl1* leads to the formation of EA/TEF accompanied by lung lobe fusion. Co-existence of EA/TEF and lung lobation defects is common in both human patients and mouse genetic models. For example, deletion of genes including *Nkx2.1*, *Shh* and its downstream targets *Glis* results in abnormal separation and lobation defects (Litingtung et al., 1998; Minoo et al., 1999; Motoyama et al., 1998). Our analysis further revealed that Isl1 regulates the transcription of *Nkx2.1*, and that *Isl1* deletion leads to the reduced expression of *Nkx2.1* in the foregut including the lung progenitor cells. Nkx2.1 is known to regulate the differentiation of multiple lung lineages including alveolar epithelium (SpC+), in addition to trachea-esophageal separation (Bohinski et al., 1994; Minoo et al., 2007). Our data suggest that Isl1 regulation of Nkx2.1 is critical for lung lobation, but not for lung epithelial differentiation. This is consistent with the transient expression of Isl1 which persists until late E13.5, prior to the initiation of epithelial differentiation in the developing lung (Morrisey and Hogan, 2010). Therefore, it is possible that Nkx2.1 is regulated by other transcription factors or signaling molecules during alveolar differentiation.

In summary, our findings provide direct genetic evidence that *Isl1* gene mutation underlies the formation of EA/TEF. We further determined the underlying cellular mechanisms and identified an epithelial progenitor population (MEC) that plays a critical role in mediating trachea-esophageal separation. We demonstrated that Isl1 regulates the transcription of Nkx2.1 in this unique population. It is noteworthy that chromosomal deletions at 5q11.2 encompassing the *ISL1* gene (and other genes) are found in patients with abnormal trachea-esophageal separation (de Jong et al., 2010). Now our studies provide definitive evidence that *ISL1* is the key gene in this chromosomal region regulating foregut morphogenesis. These findings offer opportunities for early diagnosis and intervention of EA/TEF and associated lung abnormalities.

Lead Contact and Materials Availability

Further information and requests for resources and reagents should be directed to and will be fulfilled by the Lead Contact, Jianwen Que (jq2240@cumc.columbia.edu). This study did not generate any new unique reagents.

Experimental Model and Subject Details

Mice

All animal experiments were conducted in accordance with procedures approved by the Institutional Animal Care and Use Committee at Columbia University and the University of Rochester. The *Shh-Cre*, *Sox2-CreER*, *Nkx2.1-CreER, Dermo1-Cre, Isl1loxp* and *R26-lacZ* (*Gt(ROSA)26Sor*^{tm1Sor}) mouse lines were previously described (Arnold et al., 2011; Harfe et al., 2004; Pan et al., 2008; Soriano, 1999; Taniguchi et al., 2011; Yu et al., 2003). C57BL/6 wildtype mice were purchased from Jackson Laboratory. To lineage trace Sox2^{+}

and Nkx2.1^{+} cells, female mice carrying *Sox2-CreER;R26-LacZ* and *Nkx2.1-CreER;R26-LacZ* embryos were injected with Tamoxifen (0.1mg/g body weight) intraperitoneally at E8.5 and E9.5. To delete *Isl1* in the midline epithelium of the foregut, female mice carrying *Sox2-CreER;Isl1$^{loxp/loxp}$* embryos were injected with Tamoxifen (0.1mg/g body weight) intraperitoneally at E8.5.

Xenopus—*X. laevis* embryos were obtained and raised at the *X. laevis* research resource for immunology at the University of Rochester (https://www.urmc.rochester.edu/microbiology-immunology/xenopus-laevis.aspx) using standard procedures and staged according to Nieuwkoop and Faber (1967). The antisense morpholino oligonucleotides (MOs) for *X. laevis* were obtained from Gene Tools, LLC. Morpholinos (10 ng) were injected into 16 cells stage *X. laevis* embryos and analyzed at stage 41. Morpholinos are listed in the Key Resources Table. All experiments were repeated at least three independent times with similar results.

METHOD DETAILS

Tissue preparation, Histology and Immunostaining

Tissues (mouse and *X. laevis*) processing and immunostaining were performed as previously described (Hou et al., 2019; Jiang et al., 2017; Rankin et al., 2016; Zhang et al., 2018). Briefly, samples were harvested in PBS and fixed in 4% paraformaldehyde at 4°C overnight. After fixation, samples were dehydrated with ethanol and embedded in paraffin for sectioning. 7 μm sections were cut from paraffin-embedded blocks. The primary antibodies used for immunostaining include: mouse anti-Isl1 (1:50, Developmental Studies Hybridoma Bank, 40.2D6); goat anti-Isl1 (1:200, R&D Systems, AF1837); mouse anti-p63 (1:500, Biocare Medical, CM163B), rabbit anti-Nkx2.1 (1:500, Abcam, ab76013); rat anti-Sox2 (1:250, Thermo Fisher Scientific, 14-9811-82); goat anti-Sox9 (1:200, R&D Systems, AF3075); rabbit anti-pHH3 (1:250, Sigma-Aldrich, H9908); mouse anti-CC10 (1:200, Santa Cruz Biotechnology, sc-365992); mouse anti-Acetylated Tubulin (1:100, Sigma-Aldrich, T7451); hamster anti-T1α (1:200, Developmental Studies Hybridoma Bank, 8.1.1); rabbit anti-SPC (1:200, Abcam, ab90716). Fluorescent secondary antibodies used for detection and visualization include: donkey anti-mouse IgG Alexa Fluor 488 (A-21202); donkey anti-rat IgG Alexa Fluor 488 (A-21208); donkey anti-rabbit IgG Alexa Fluor 488 (A-21206); donkey anti-rabbit IgG Alexa Fluor 555 (A-31572); donkey anti-mouse IgG Alexa Fluor 555 (A-31570); goat anti-hamster IgG Alexa Fluor 546 (A-21111); donkey anti-rabbit IgG Alexa Fluor 647 (A-31573); all from Thermo Fisher Scientific. For Hematoxylin and Eosin staining, paraffin sections were deparaffinized and rehydrated. Sections were treated with Mayer's Hematoxylin for 1 minute, followed by treated with Alcoholic-Eosin for 1 minute. Images were obtained using a Nikon SMZ1500 Inverted microscope (Nikon). Confocal images were obtained with a Zeiss LSM 710 confocal laser-scanning microscope (Carl Zeiss).

Whole-mount Staining

Whole-mount stating was performed as previously described (Que et al., 2006). Tissue samples were fixed in 4% paraformaldehyde at 4°C for 30 minutes. Tissues were blocked for

1 hour with blocking solution and incubated with rat anti-E-cadherin primary antibody (1:1000, Sigma-Aldrich, U3254), followed by incubation with biotinylated or fluorescent secondary antibody at room temperature. Tissues that were incubated with biotinylated secondary antibody were incubated with avidin-biotin-peroxidase complex (Vector Laboratories, PK-4000) and incubated in DAB solution (Vector Laboratories, SK-4100).

X-gal Staining

The trachea, esophagus, and embryos were fixed in 4% paraformaldehyde at 4° for 30 minutes, followed by X-gal staining overnight at 37°C. X-gal-stained samples were postfixed in 4% PFA at 4°C overnight, and dehydrated with ethanol and embedded in paraffin for sectioning.

Cell Culture and Luciferase Assay

The mouse lung epithelial cell line MLE-15 was provided by Dr. Jining Lu in the Department of Medicine, Columbia University. The pancreatic beta cell line HIT-T15 was purchased from ATCC. Cells were cultured in RPMI 1640 medium (Thermo Fisher Scientific) supplemented with 10% FBS. The pCMV-Isl1 plasmid was purchased from OriGene. To test whether the *Nkx2.1* promoter is regulated by *Isl1*, a 0.4 kb promoter region of the *Nkx2.1* gene was cloned into the pGL3 luciferase report vector, and then co-transfected into cells with pCMV-YFP or pCMV-Isl1 plasmids. The following primers were used: forward, 5’-CGTGAAGGTACCCTCTCTTTGAGACCTAAA-3’; reverse, 5’-GCAAGTCTCGAGACATGATTCGGCGTCGGC-3’. Point mutation of the potential binding sites was generated by site-directed mutagenesis using GeneArt Site-Directed Mutagenesis Kit (Thermo Fisher Scientific) with the following primers: forward, 5’-GTCATCAGCATGTAAGCTAATTATCTCGGGCAAGATGT-3’; reverse, 5’-ACATCTTGCCCGAGATACGGCGCTTACATGCTGATGAC-3’. Luciferase activity was determined 48 hours after transfection using the Dual-Luciferase Reporter Assay Kit (Promega) and the GloMax-Multi Detection System (Promega).

Microarray Analysis

Total RNA was extracted from pooled tracheas or esophagi of E11.5 C57BL/6 wildtype embryos with RNeasy Micro Kit (Qiagen), and RNA quality was checked with a 2100 Bioanalyzer (Agilent Technologies). Three paired RNA samples for trachea and esophagus was amplified and labeled using the Ovation RNA Amplification Kit V2 and FL-Ovation Biotin V2 (NuGEN) by the Duke Microarray Facility. Standard Affymetrix protocols and mouse genomic 430 2.0 chips were used. The array datasets were imported into Bioconductor in the R software environment and preprocessed using robust multichip averaging. Calculation of fold change and t tests was performed for each probe set between the trachea and esophagus groups, and fold change >1.5 were annotated.

Quantitative Real-Time Polymerase Chain Reaction

The tracheas and esophagi were isolated from E11.5 wild type embryos. RNA was isolated using the PicoPure RNA Isolation Kit (Thermo Fisher Scientific), and RNA reverse transcription was performed using the SuperScript IV First-Strand Synthesis Kit (Invitrogen)

according to the manufacturer's instructions. cDNA was subjected to quantitative real-time polymerase chain reaction (qPCR) using the StepOnePlus Real-Time PCR Detection System (Applied Biosystems) and iTaq Universal SYBR Green Supermix (Bio-Rad). The primers used for qPCR are listed in the Key Resources Table. The transcript levels of genes were normalized to beta-actin expression. All qPCR experiments were performed in triplicate.

Chromatin Immunoprecipitation Assay

For chromatin immunoprecipitation assay, the small cell lung cancer cell line H1882 was purchased from ATCC. ChIP assay was performed as previously described using Pierce Agarose ChIP Kit (Thermo Fisher Scientific) with minor modifications (Huang et al., 2015). Briefly, the cells were cross-linked with 1% formaldehyde for 10 min at room temperature, followed by adding 1X Glycine Solution to quench the cross-linking reaction. After two washes with ice-cold PBS, the cells were detached by scraping and collected and stored for later use or directly lysed with Lysis Buffer 1. Cell lysate was centrifuged at 9000x g for 3 min to pellet the nuclei, which were then resuspended in MNase Digestion Buffer. Micrococcal Nuclease (New England Biolabs) was added to digest the DNA to an average size of ~500 bp at 37°C. MNase Stop Solution was then added and incubated on ice for 5 min. The nuclei were spun down again and resuspended in Lysis Buffer 2. After incubation for 15 min on ice, the samples were centrifuged at 9000x g for 5 min to remove the cellular debris. The supernatant was split into halves and incubated with 5ug of Isl1 antibody (R&D Systems, AF1837) or control goat IgG antibody (R&D Systems, AB-108-C) overnight at 4°C on a rocking platform. 20 ul of protein A/G beads were added to each sample for incubation for 1hr at 4°C with rocking. Beads were collected and washed once with IP Wash Buffer 1, twice with IP Wash Buffer 2 and once with IP Wash Buffer 3. Protease inhibitors were added for the above steps as indicated in the manufacturer's instruction. Immunoprecipitated protein-DNA complexes were eluted with IP Elution Buffer at 65°C for 30–40min. Then protein was digested by adding 2ul of 20 ug/ml Proteinase K (Thermo Fisher Scientific) to each sample in the presence of 0.2M NaCl at 65°C for 1.5hrs. DNA was recovered using the DNA clean-up columns in the Kit and used for qPCR analysis with a primer set for amplifying the regulatory region of *Nkx2.1* (forward, 5'-GCCTCCACTCAAGCCAATTA-3'; reverse, 5'-TCGTGTGCTTTGGACTCATC-3'). The *GAPDH* primers from the Kit were used as a negative control.

Quantification and Statistical Analysis

Quantification of Proliferation—After immunostaining for pHH3, images were taken with a DMi8 inverted microscopes (Leica Microsystems). The total number of epithelial cells (DAPI positive) and the number of pHH3 positive nuclei in the foregut epithelium were counted on transverse sections of four controls and six *Shh-Cre;Isl1*$^{loxp/loxp}$ mutants at E9.5 and three controls and three mutants at E10.5 using ImageJ software. The percentage was obtained by dividing the number of pHH3 positive cells by the total number of epithelial cells and multiplying by 100.

Statistics—Quantitative data are presented as the mean ± SEM. Statistical significance was determined by Student's t-tests, and p-values of < 0.05 were considered statistically significant. For all graphs, asterisks represent statistical significance at the following levels:

*p < 0.05, **p < 0.01, ***p < 0.001, whereas NS denotes not significant. All data were analyzed using GraphPad Prism statistical software.

Data and Software Availability

Further information and requests for the datasets generated during this study should be directed to the Lead Contact Dr. Jianwen Que.

Supplementary Material

Refer to Web version on PubMed Central for supplementary material.

Acknowledgements

We thank Tina Martin and Francisco De Jesus Andino for animal husbandry. We are grateful for the funds provided by NIH (R01HL132996, R01DK100342 (J.Q)), R24AI059830 (J.R)) and the National Science Foundation (J.R).

Reference:

Ahlgren U, Pfaff SL, Jessell TM, Edlund T, and Edlund H (1997). Independent requirement for ISL1 in formation of pancreatic mesenchyme and islet cells. Nature 385, 257–260. [PubMed: 9000074]

Arnold K, Sarkar A, Yram MA, Polo JM, Bronson R, Sengupta S, Seandel M, Geijsen N, and Hochedlinger K (2011). Sox2(+) adult stem and progenitor cells are important for tissue regeneration and survival of mice. Cell Stem Cell 9, 317–329. [PubMed: 21982232]

Behrens C, and Yen PP (2011). Esophageal inlet patch. Radiol Res Pract 2011, 460890. [PubMed: 22091379]

Bohinski RJ, Di Lauro R, and Whitsett JA (1994). The lung-specific surfactant protein B gene promoter is a target for thyroid transcription factor 1 and hepatocyte nuclear factor 3, indicating common factors for organ-specific gene expression along the foregut axis. Molecular and cellular biology 14, 5671–5681. [PubMed: 8065304]

Bu L, Jiang X, Martin-Puig S, Caron L, Zhu S, Shao Y, Roberts DJ, Huang PL, Domian IJ, and Chien KR (2009). Human ISL1 heart progenitors generate diverse multipotent cardiovascular cell lineages. Nature 460, 113–117. [PubMed: 19571884]

Cai CL, Liang X, Shi Y, Chu PH, Pfaff SL, Chen J, and Evans S (2003). Isl1 identifies a cardiac progenitor population that proliferates prior to differentiation and contributes a majority of cells to the heart. Dev Cell 5, 877–889. [PubMed: 14667410]

Cho HH, Cargnin F, Kim Y, Lee B, Kwon RJ, Nam H, Shen R, Barnes AP, Lee JW, Lee S, et al. (2014). Isl1 directly controls a cholinergic neuronal identity in the developing forebrain and spinal cord by forming cell type-specific complexes. PLoS genetics 10, e1004280. [PubMed: 24763339]

de Jong EM, Douben H, Eussen BH, Felix JF, Wessels MW, Poddighe PJ, Nikkels PG, de Krijger RR, Tibboel D, and de Klein A (2010). 5q11.2 deletion in a patient with tracheal agenesis. Eur J Hum Genet 18, 1265–1268. [PubMed: 20551993]

Di Nardo G, Cremon C, Bertelli L, Oliva S, De Giorgio R, and Pagano N (2016). Esophageal Inlet Patch: An Under-Recognized Cause of Symptoms in Children. J Pediatr 176, 99–104 e101. [PubMed: 27318379]

Domyan ET, Ferretti E, Throckmorton K, Mishina Y, Nicolis SK, and Sun X (2011). Signaling through BMP receptors promotes respiratory identity in the foregut via repression of Sox2. Development 138, 971–981. [PubMed: 21303850]

Fausett SR, Brunet LJ, and Klingensmith J (2014). BMP antagonism by Noggin is required in presumptive notochord cells for mammalian foregut morphogenesis. Dev Biol 391, 111–124. [PubMed: 24631216]

Fragoso AC, and Tovar JA (2014). The multifactorial origin of respiratory morbidity in patients surviving neonatal repair of esophageal atresia. Front Pediatr 2, 39. [PubMed: 24829898]

Goss AM, Tian Y, Tsukiyama T, Cohen ED, Zhou D, Lu MM, Yamaguchi TP, and Morrisey EE (2009). Wnt2/2b and beta-catenin signaling are necessary and sufficient to specify lung progenitors in the foregut. Dev Cell 17, 290–298. [PubMed: 19686689]

Harfe BD, Scherz PJ, Nissim S, Tian H, McMahon AP, and Tabin CJ (2004). Evidence for an expansion-based temporal Shh gradient in specifying vertebrate digit identities. Cell 118, 517–528. [PubMed: 15315763]

Harris-Johnson KS, Domyan ET, Vezina CM, and Sun X (2009). beta-Catenin promotes respiratory progenitor identity in mouse foregut. Proc Natl Acad Sci U S A 106, 16287–16292. [PubMed: 19805295]

Hines EA, Jones MK, Verheyden JM, Harvey JF, and Sun X (2013). Establishment of smooth muscle and cartilage juxtaposition in the developing mouse upper airways. Proc Natl Acad Sci U S A 110, 19444–19449. [PubMed: 24218621]

Hou Z, Wu Q, Sun X, Chen H, Li Y, Zhang Y, Mori M, Yang Y, Que J, and Jiang M (2019). Wnt/Fgf crosstalk is required for the specification of basal cells in the mouse trachea. Development 146.

Huang H, Santoso N, Power D, Simpson S, Dieringer M, Miao H, Gurova K, Giam CZ, Elledge SJ, and Zhu J (2015). FACT Proteins, SUPT16H and SSRP1, Are Transcriptional Suppressors of HIV-1 and HTLV-1 That Facilitate Viral Latency. J Biol Chem 290, 27297–27310. [PubMed: 26378236]

Jen Y, Manova K, and Benezra R (1996). Expression patterns of Id1, Id2, and Id3 are highly related but distinct from that of Id4 during mouse embryogenesis. Dev Dyn 207, 235–252. [PubMed: 8922523]

Jiang M, Li H, Zhang Y, Yang Y, Lu R, Liu K, Lin S, Lan X, Wang H, Wu H, et al. (2017). Transitional basal cells at the squamous-columnar junction generate Barrett's oesophagus. Nature 550, 529–533. [PubMed: 29019984]

Legrand C, Michaud L, Salleron J, Neut D, Sfeir R, Thumerelle C, Bonnevalle M, Turck D, and Gottrand F (2012). Long-term outcome of children with oesophageal atresia type III. Arch Dis Child 97, 808–811. [PubMed: 22753768]

Li Y, Litingtung Y, Ten Dijke P, and Chiang C (2007). Aberrant Bmp signaling and notochord delamination in the pathogenesis of esophageal atresia. Dev Dyn 236, 746–754. [PubMed: 17260385]

Litingtung Y, Lei L, Westphal H, and Chiang C (1998). Sonic hedgehog is essential to foregut development. Nat Genet 20, 58–61. [PubMed: 9731532]

Malmstrom K, Lohi J, Lindahl H, Pelkonen A, Kajosaari M, Sarna S, Malmberg LP, and Makela MJ (2008). Longitudinal follow-up of bronchial inflammation, respiratory symptoms, and pulmonary function in adolescents after repair of esophageal atresia with tracheoesophageal fistula. J Pediatr 153, 396–401. [PubMed: 18534205]

Minoo P, Hu L, Xing Y, Zhu NL, Chen H, Li M, Borok Z, and Li C (2007). Physical and functional interactions between homeodomain NKX2.1 and winged helix/forkhead FOXA1 in lung epithelial cells. Molecular and cellular biology 27, 2155–2165. [PubMed: 17220277]

Minoo P, Su G, Drum H, Bringas P, and Kimura S (1999). Defects in tracheoesophageal and lung morphogenesis in Nkx2.1(−/−) mouse embryos. Dev Biol 209, 60–71. [PubMed: 10208743]

Moretti A, Caron L, Nakano A, Lam JT, Bernshausen A, Chen Y, Qyang Y, Bu L, Sasaki M, Martin-Puig S, et al. (2006). Multipotent embryonic isl1+ progenitor cells lead to cardiac, smooth muscle, and endothelial cell diversification. Cell 127, 1151–1165. [PubMed: 17123592]

Morrisey EE, and Hogan BL (2010). Preparing for the first breath: genetic and cellular mechanisms in lung development. Dev Cell 18, 8–23. [PubMed: 20152174]

Motoyama J, Liu J, Mo R, Ding Q, Post M, and Hui CC (1998). Essential function of Gli2 and Gli3 in the formation of lung, trachea and oesophagus. Nat Genet 20, 54–57. [PubMed: 9731531]

Pan L, Deng M, Xie X, and Gan L (2008). ISL1 and BRN3B co-regulate the differentiation of murine retinal ganglion cells. Development 135, 1981–1990. [PubMed: 18434421]

Que J (2015). The initial establishment and epithelial morphogenesis of the esophagus: a new model of tracheal-esophageal separation and transition of simple columnar into stratified squamous epithelium in the developing esophagus. Wiley interdisciplinary reviews Developmental biology.

Que J, Choi M, Ziel JW, Klingensmith J, and Hogan BL (2006). Morphogenesis of the trachea and esophagus: current players and new roles for noggin and Bmps. Differentiation 74, 422–437. [PubMed: 16916379]

Que J, Luo X, Schwartz RJ, and Hogan BL (2009). Multiple roles for Sox2 in the developing and adult mouse trachea. Development 136, 1899–1907. [PubMed: 19403656]

Que J, Okubo T, Goldenring JR, Nam KT, Kurotani R, Morrisey EE, Taranova O, Pevny LH, and Hogan BL (2007). Multiple dose-dependent roles for Sox2 in the patterning and differentiation of anterior foregut endoderm. Development 134, 2521–2531. [PubMed: 17522155]

Rajagopal J, Carroll TJ, Guseh JS, Bores SA, Blank LJ, Anderson WJ, Yu J, Zhou Q, McMahon AP, and Melton DA (2008). Wnt7b stimulates embryonic lung growth by coordinately increasing the replication of epithelium and mesenchyme. Development 135, 1625–1634. [PubMed: 18367557]

Rankin SA, Han L, McCracken KW, Kenny AP, Anglin CT, Grigg EA, Crawford CM, Wells JM, Shannon JM, and Zorn AM (2016). A Retinoic Acid-Hedgehog Cascade Coordinates Mesoderm-Inducing Signals and Endoderm Competence during Lung Specification. Cell Rep 16, 66–78. [PubMed: 27320915]

Rankin SA, Thi Tran H, Wlizla M, Mancini P, Shifley ET, Bloor SD, Han L, Vleminckx K, Wert SE, and Zorn AM (2015). A Molecular atlas of Xenopus respiratory system development. Dev Dyn 244, 69–85. [PubMed: 25156440]

Shu W, Jiang YQ, Lu MM, and Morrisey EE (2002). Wnt7b regulates mesenchymal proliferation and vascular development in the lung. Development 129, 4831–4842. [PubMed: 12361974]

Sistonen S, Malmberg P, Malmstrom K, Haahtela T, Sarna S, Rintala RJ, and Pakarinen MP (2010). Repaired oesophageal atresia: respiratory morbidity and pulmonary function in adults. Eur Respir J 36, 1106–1112. [PubMed: 20351029]

Soriano P (1999). Generalized lacZ expression with the ROSA26 Cre reporter strain. Nat Genet 21, 70–71. [PubMed: 9916792]

Taniguchi H, He M, Wu P, Kim S, Paik R, Sugino K, Kvitsiani D, Fu Y, Lu J, Lin Y, et al. (2011). A resource of Cre driver lines for genetic targeting of GABAergic neurons in cerebral cortex. Neuron 71, 995–1013. [PubMed: 21943598]

Tata PR, Chow RD, Saladi SV, Tata A, Konkimalla A, Bara A, Montoro D, Hariri LP, Shih AR, Mino-Kenudson M, et al. (2018). Developmental History Provides a Roadmap for the Emergence of Tumor Plasticity. Dev Cell 44, 679–693 e675. [PubMed: 29587142]

Wales PW, Drab SA, Connolly B, and Kim PC (2002). Horseshoe lung in association with other foregut anomalies: what is the significance? Journal of pediatric surgery 37, 1205–1207. [PubMed: 12149704]

Yu K, Xu J, Liu Z, Sosic D, Shao J, Olson EN, Towler DA, and Ornitz DM (2003). Conditional inactivation of FGF receptor 2 reveals an essential role for FGF signaling in the regulation of osteoblast function and bone growth. Development 130, 3063–3074. [PubMed: 12756187]

Zhang Y, Jiang M, Kim E, Lin S, Liu K, Lan X, and Que J (2016). Development and stem cells of the esophagus. Seminars in cell & developmental biology.

Zhang Y, Yang Y, Jiang M, Huang SX, Zhang W, Al Alam D, Danopoulos S, Mori M, Chen YW, Balasubramanian R, et al. (2018). 3D Modeling of Esophageal Development using Human PSC-Derived Basal Progenitors Reveals a Critical Role for Notch Signaling. Cell Stem Cell 23, 516–529 e515. [PubMed: 30244870]

Highlights:

1. *Isl1* disruption leads to abnormal tracheo-esophageal separation in frog and mouse
2. Nkx2.1 lineage-derived respiratory cells contribute to the esophageal epithelium.
3. A midline cell population is critical for tracheo-esophageal separation.
4. Isl1 regulates the transcription of Nkx2.1 in the midline epithelial progenitor cells.

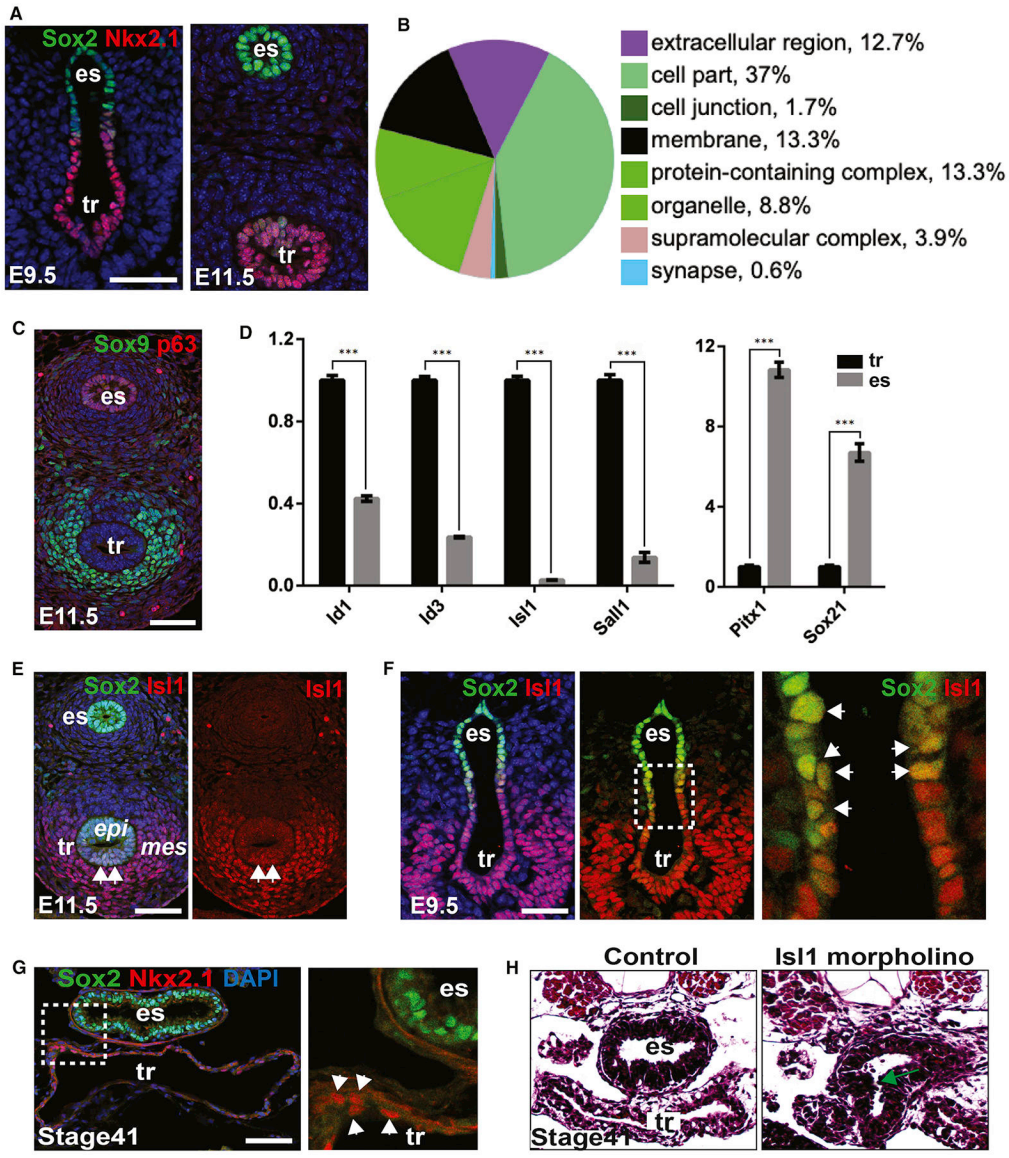

Figure 1. *Isl1* is differentially expressed in the dorsal-ventral region of the early mouse foregut and required for trachea-esophageal separation in *Xenopus laevis*.

(A) Sox2 and Nkx2.1 maintain differential expression pattern in the early mouse foregut (E9.5-E11.5). **(B)** Genes differentially expressed in E11.5 mouse trachea and esophagus are involved in multiple cellular functions as revealed by PANTHER (Protein Analysis Through Evolutionary Relationships). **(C)** p63 and Sox9 are enriched in the E11.5 esophagus and trachea, respectively. **(D)** qPCR confirms differentially expressed genes in the E11.5 trachea and esophagus. **(E)** Isl1 expression is enriched in the epithelium (arrows) and mesenchyme of the trachea but not esophagus at E11.5. Note the levels of Isl1 are low in the epithelium compared to the mesenchyme. **(F)** Isl1 is enriched in the ventral epithelium and mesenchyme of the mouse foregut at E9.5. Note the co-localization of Sox2 and Isl1 in the dorsal-ventral boundary cells (arrowheads). **(G)** Sox2 and Nkx2.1 (arrowheads) are enriched in the esophagus and trachea of *X. laevis* at stage 41. **(H)** Morpholino-mediated knockdown of Isl1 in *X. laevis* embryos leads to abnormal trachea-esophageal separation (arrow)

(n=8/14). Abbreviation: es, esophagus; tr, trachea; epi, epithelium; mes, mesenchyme. Scale bar: 50μm. See also Figure S1.

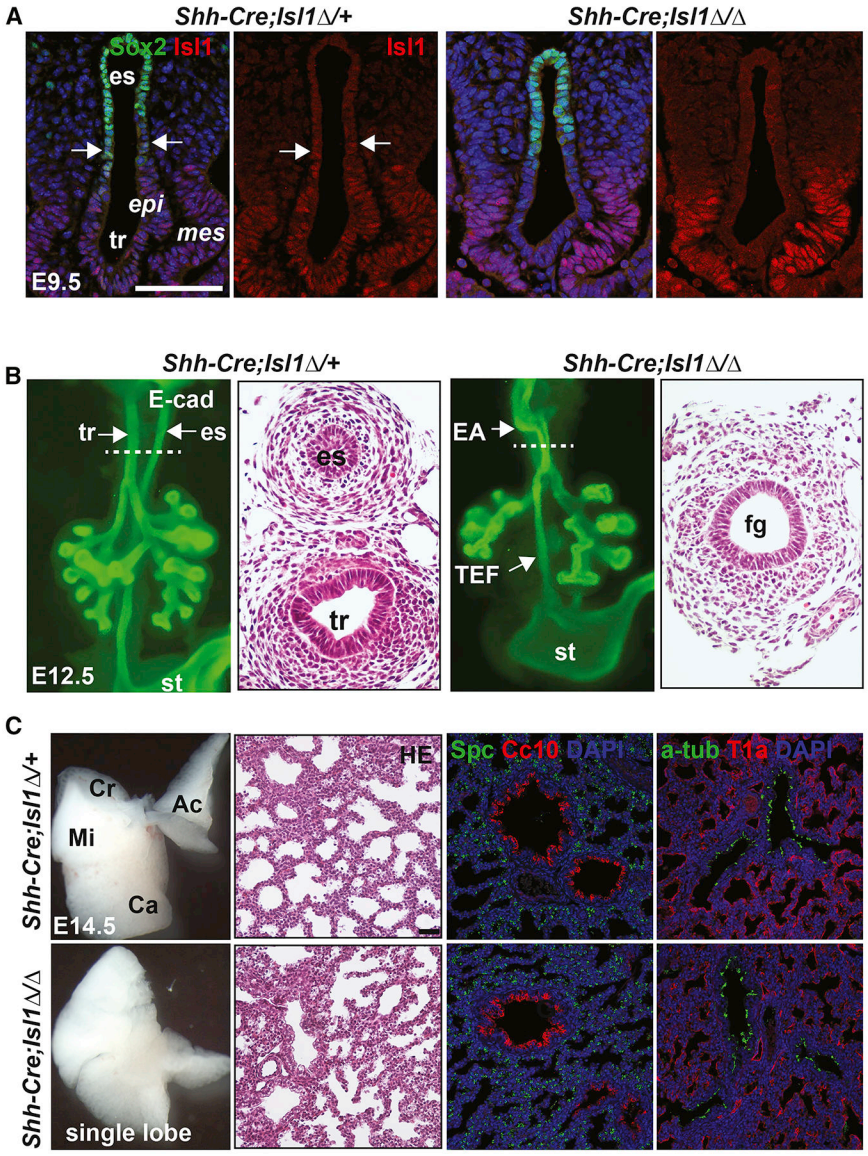

Figure 2. Deletion of *Isl1* leads to EA/TEF and fusion of right lung lobes.

(A) Isl1 expression is lost in the foregut epithelium but not mesenchyme of *Shh-Cre; Isl1*$^{loxp/loxp}$ mutants. **(B)** *Isl1* deletion causes EA/TEF formation in approximately 50% mutants (n=18/36). **(C)** *Isl1* deletion results in fusion of all four right lung lobes in all *Shh-Cre; Isl1*$^{loxp/loxp}$ mutants (n=36/36). Note expression of airway/alveolar epithelium markers seems unperturbed in the mutant lung (n=5). Abbreviation: Cr, cranial lobe; Ac, accessory lobe; Mi, middle lobe; Ca, caudal lobe. Scale bar: 50μm. See also Figure S2 and S3.

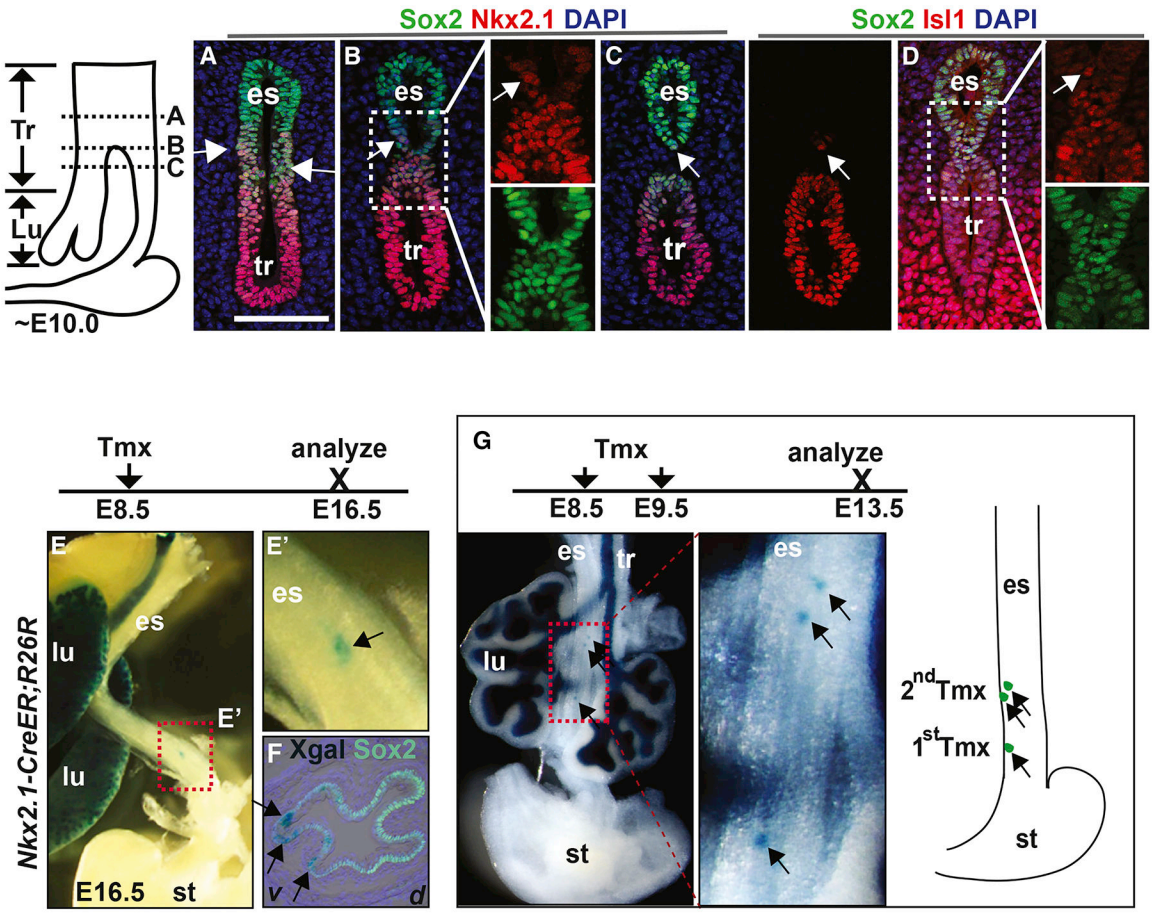

Figure 3. Nkx2.1+ lineage derived cells contribute to the esophagus.

(A) The epithelium at the dorsal-ventral boundary (arrows) co-expresses Sox2 and Nkx2.1. **(B)** Sox2+ Nkx2.1+ epithelial cells (arrow) are present in the septum and forming esophagus. **(C)** Presence of a few Sox2+ Nkx2.1+ epithelial cells (arrow) in the ventral epithelium of the nascent esophagus. **(D)** Sox2+ Isl1+ epithelial cells (arrow) are present in the septum and forming esophagus. **(E-G)** *Nkx2.1-CreER* lineage labeled cells contribute to the ventral epithelium (arrows) of the esophagus. While a single dose of Tamoxifen induces Xgal+ cells in one location, two doses of Tamoxifen induce Xgal+ cells in two separate locations (G). Abbreviation: v, ventral; d, dorsal; Tmx, tamoxifen. Scale bar: 50μm. See also Figure S4.

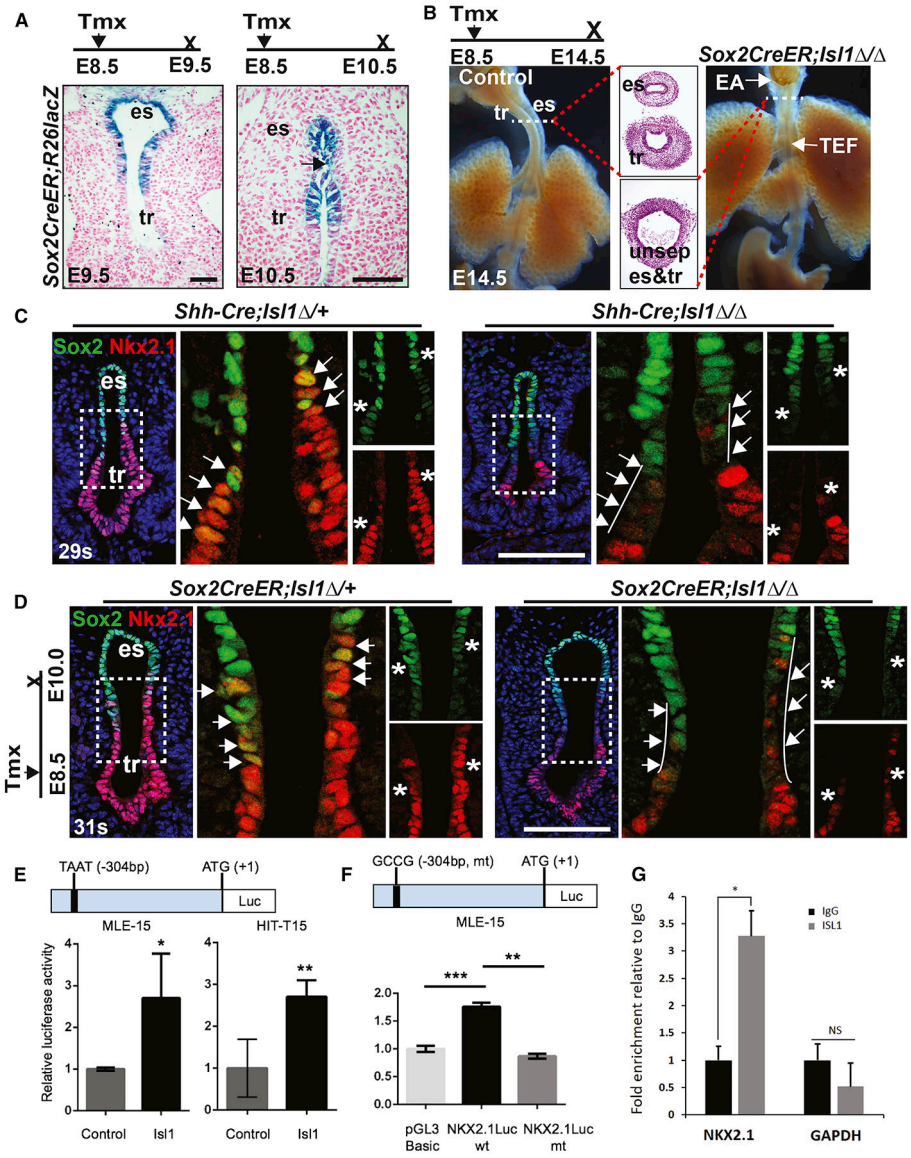

Figure 4. Isl1 regulation of Nkx2.1 in the boundary population is critical for trachea-esophageal separation.

(A) Upon a single low dose of Tmx injection at E8.5, *Sox2-CreER* lineage labeled cells are present in the dorsal and midline of the foregut at E9.5. At E10.5 lineage labeled cells are present in the esophagus and forming dorsal trachea. **(B)** Deletion of *Isl1* with *Sox2-CreER* leads to EA/TEF in all mutants (n=9). Samples were immunostained with an anti E-cadherin antibody. **(C-D)** *Isl1* deletion results in decreased levels of Nkx2.1 in *Shh-Cre;Isl1*$^{loxp/loxp}$ and *Sox2-CreER;Isl1*$^{loxp/loxp}$ mutants. Note the decreased levels of Nkx2.1 in the midline cells (arrows and stars) and some ventral epithelial cells also exhibit reduced levels of Nkx2.1. **(E-F)** The Isl1 binding site (TAAT) is critical for the regulation of Nkx2.1 transcription as shown by luciferase assays. Mutation of the site abolishes the regulation. Note that cell lines were co transfected with Isl1 plasmids. **(G)** Enrichment of Isl1 binding to the *Nkx2.1* locus as shown by ChIP-qPCR. Scale bar: 50μm. See also Figure S4.

Table 1.

The transcript levels of the transcription factors that are up- or downregulated by >1.5-fold in the E11.5 esophagus Vs trachea

Upregulated in esophagus		Downregulated in esophagus	
Gene	**Log_2 fold change**	**Gene**	**Log_2 fold change**
Sox21	7.58	*Sox9*	−2.02
Myocd	6.14	*Id3*	−2.41
Pitxl	5.92	*Foxc2*	−2.49
Trp63	5.69	*Id1*	−2.72
Foxd1	4.72	*Tbx5*	−2.75
Nkx6–1	4.05	*Lhx6*	−2.76
Meox2	3.96	*Hoxa5*	−3.38
Pitx2	3.95	*Tbx3*	−3.94
Irf6	3.79	*Tbx2*	−4.45
Sox2	3.03	*Sall1*	−5.02
Klf4	2.46	*Irx2*	−6.71
Foxf2	2.27	*Esrrb*	−7.25
Foxp1	2.2	*Isl1*	−7.7
Klf5	2.06	*Myog*	−43.43
Hic1	1.87		
Snai2	1.82		
Atbf1	1.72		
Foxa2	1.71		

Key Resources Table

REAGENT or RESOURCE	SOURCE	IDENTIFIER
Antibodies		
Mouse monoclonal anti-p63	Biocare Medical	Cat# CM163B; RRID: AB_10583039
Rat monoclonal anti-E-cadherin	Sigma-Aldrich	Cat#U3254; RRID: AB 477600
Rabbit monoclonal anti-Nkx2.1	Abcam	Cat#ab76013; RRID: AB_1310784
Rat monoclonal anti-Sox2	Thermo Fisher Scientific	Cat#14-9811-82; RRID: AB_11219471
Goat polyclonal anti-Sox9	R&D Systems	Cat#AF3075; RRID: AB_2194160
Goat polyclonal anti-Isl1	R&D Systems	Cat#AF1837; RRID: AB_2126324
Mouse monoclonal anti-Isl1	Developmental Studies Hybridoma Bank	Cat#40.2D6; RRID: AB_528315
Rabbit polyclonal anti-pHH3	Sigma-Aldrich	Cat#H9908; RRID: AB_260096
Mouse monoclonal anti-CC10 (E-11)	Santa Cruz Biotechnology	Cat#sc-365992; RRID: AB_10915481
Mouse monoclonal anti-Acetylated tubulin	Sigma-Aldrich	Cat#T7451; RRID:AB_609894
Hamster monoclonal anti-T1α	Developmental Studies Hybridoma Bank	Cat#8.1.1; RRID: AB_531893
Rabbit polyclonal anti-SPC	Abcam	Cat#ab90716; RRID: AB_10674024
Goat polyclonal anti-IgG	R&D Systems	Cat#AB-108-C; RRID: AB_354267
Donkey anti-mouse IgG Alexa Fluor 488	Thermo Fisher Scientific	Cat#A-21202; RRID: AB_141607
Donkey anti-rat IgG Alexa Fluor 488	Thermo Fisher Scientific	Cat#A-21208; RRID: AB_141709
Donkey anti-rabbit IgG Alexa Fluor 488	Thermo Fisher Scientific	Cat#A-21206; RRID: AB_2535792
Donkey anti-mouse IgG Alexa Fluor 555	Thermo Fisher Scientific	Cat#A-31570; RRID: AB_2536180
Donkey anti-goat IgG Alexa Fluor 555	Thermo Fisher Scientific	Cat#A-21432; RRID: AB_2535853
Goat anti-hamster IgG Alexa Fluor 546	Thermo Fisher Scientific	Cat#A-21111; RRID: AB_2535760
Donkey anti-rabbit IgG Alexa Fluor 647	Thermo Fisher Scientific	Cat#A-31573; RRID: AB_2536183
Chemicals, Peptides, and Recombinant Proteins		
RPMI 1640	Thermo Fisher Scientific	Cat#11875119
DAPI	Sigma-Aldrich	Cat#D9542
Micrococcal Nuclease	New England Biolabs	Cat#M0247S
Proteinase K	Thermo Fisher Scientific	Cat#26160
Tamoxifen	Sigma-Aldrich	Cat#T5648
Critical Commercial Assays		
SuperScript IV First-Strand Synthesis System	Invitrogen	Cat#18091050
Dual-Luciferase Reporter Assay System	Promega	Cat#E1910
GeneArt Site-Directed Mutagenesis System	Thermo Fisher Scientific	Cat#A13282
PicoPure RNA Isolation Kit	Thermo Fisher Scientific	Cat#KIT0204
RNeasy Micro Kit	Qiagen	Cat#74004
Pierce Agarose ChIP Kit	Thermo Fisher Scientific	Cat#26156
Deposited Data		

REAGENT or RESOURCE	SOURCE	IDENTIFIER
Microarray data of E11.5 mouse trachea and esophagus	This paper	Supplemental Table 1
Experimental Models: Cell Lines		
Mouse: MLE-15	Laboratory of Jining Lu	N/A
Hamster: HIT-T15	ATCC	CRL-1777
Human: H1882	ATCC	CRL-5903
Experimental Models: Organisms/Strains		
Mouse: *Isl1$^{loxp/loxp}$*	(Pan et al., 2008)	N/A
Mouse: *Shh-Cre*	(Harfe et al., 2004)	N/A
Mouse: *Sox2-CreER*	(Arnold et al., 2011)	N/A
Mouse: *Nkx2.1-CreER*	(Taniguchi et al., 2011)	N/A
Mouse: *Dermo1-Cre*	(Yu et al., 2003)	N/A
Mouse: *R26-lacZ*	(Soriano, 1999)	N/A
Mouse: *C57BL/6*	Jackson Laboratory	JAX:000664
Xenopus laevis wild type	University of Rochester	N/A
Oligonucleotides		
Morpholino: MO-Isl1: ACTATATCAGGTACAGCAATGGGCA	Gene Tools	N/A
Morpholino: MO-Mrpl24: TCTCAGGTGCAGAAATGCGTCTGAC	Gene Tools	N/A
Morpholino: MO-Ovol2: TCTTGCCCTTTTAGTTCACAACTGG	Gene Tools	N/A
Morpholino: MO-Sall1: GCATGTCTCGGAGGAAGCAGCGAAA	Gene Tools	N/A
Primer: Id1 Forward: GCTGAACTCGGAGTCTGAAG	This paper	N/A
Primer: Id1 Reverse: GCCTCAGCGACACAAGATG	This paper	N/A
Primer: Id3 Forward: AGCTTAGCCAGGTGGAAATC	This paper	N/A
Primer: Id3 Reverse: TT GGAGATCACAAGTTCCGG	This paper	N/A
Primer: Isl1 Forward: CAGCAACCCAACGACAAAAC	This paper	N/A
Primer: Isl1 Reverse: GTCACTCAGTACTTTCCAGGG	This paper	N/A
Primer: Pitx1 Forward: GGACCAACCTCACTGAACC	This paper	N/A
Primer: Pitx1 Reverse: TGAACTGCGGCACATAGC	This paper	N/A
Primer: Sall1 Forward: GCCTCAACATTTCCAATCCG	This paper	N/A
Primer: Sall1 Reverse: ATTCAAAGAATTCAGCGCAGC	This paper	N/A
Primer: Sox21 Forward: ATGCACAACTCGGAGATCAG	This paper	N/A
Primer: Sox21 Reverse: GTACTTGTAGTCGGGATGCTC	This paper	N/A
Recombinant DNA		
Plasmid: pCMV-Isl1	OriGene	Cat#MR227038
Plasmid: pCMV-YFP	Laboratory of Jianwen Que	N/A
Plasmid: pGL3-Basic	Promega	Cat#E1751
Plasmid: Nkx2.1 Luc wt (pGL3)	This paper	N/A
Plasmid: Nkx2.1 Luc mt (pGL3)	This paper	N/A
Software and Algorithms		
ImageJ	National Institutes of Health	https://imagej.nih.gov/ij/

REAGENT or RESOURCE	SOURCE	IDENTIFIER
Prism 6	GraphPad Software	https://www.graphpad.com/scientific-software/prism/
R	Bioconductor	https://www.bioconductor.org/